



# Melting experiments on Fe–Fe<sub>3</sub>S system to 254 GPa



Yuko Mori<sup>a</sup>, Haruka Ozawa<sup>b</sup>, Kei Hirose<sup>a,\*</sup>, Ryosuke Sinmyo<sup>a</sup>, Shigehiko Tateno<sup>a,b</sup>,  
Guillaume Morard<sup>c</sup>, Yasuo Ohishi<sup>d</sup>

<sup>a</sup> Earth-Life Science Institute, Tokyo Institute of Technology, Meguro, Tokyo 152-8550, Japan

<sup>b</sup> Institute for Study of the Earth's Interior, Okayama University, Tottori 682-0193, Japan

<sup>c</sup> Institut de Minéralogie, de Physique des Matériaux et de Cosmochimie, UMR CNRS 7590, Sorbonne Universités – Université Pierre et Marie Curie, CNRS, Muséum National d'Histoire Naturelle, IRD, 4 Place Jussieu, 75005 Paris, France

<sup>d</sup> Japan Synchrotron Radiation Research Institute, Sayo-cho, Hyogo 679-5198, Japan

## ARTICLE INFO

### Article history:

Received 1 September 2016

Received in revised form 6 February 2017

Accepted 9 February 2017

Available online xxxx

Editor: J. Brodholt

### Keywords:

core  
sulfur  
melting  
eutectic liquid  
high-pressure  
diamond-anvil cell

## ABSTRACT

Melting experiments were performed on the Fe–Fe<sub>3</sub>S system at high pressures between 34 and 254 GPa in a laser-heated diamond-anvil cell (DAC), using starting materials of fine-grained homogeneous mixtures of Fe and FeS (<500 nm) prepared by induction melting and rapid quenching techniques. Melting phase relations including the liquid/solid partitioning of sulfur were examined on the basis of textural and chemical characterizations of recovered samples using a focused ion beam (FIB) and electron microprobes. The results demonstrate that the sulfur content in eutectic liquid decreases substantially with increasing pressure. The eutectic liquid Fe with 5.7(±0.3) wt.% S coexisted with both solid Fe<sub>3</sub>S and Fe containing 3.9(±0.4) wt.% S at 254 GPa and 3550 K. The eutectic liquid at inner core boundary (ICB) pressure includes less sulfur than is required to account for the density deficit of the outer core (≥10 wt.% S). Furthermore, the difference in sulfur concentration between coexisting liquid and solid is not sufficient to account for the observed density jump across the ICB. These indicate that sulfur cannot be a predominant light element in the core.

© 2017 Elsevier B.V. All rights reserved.

## 1. Introduction

Sulfur is considered to be an important light element in the Earth's core because of the low melting temperature of Fe–S alloys and its wide presence in iron meteorites (Chabot, 2004). Density measurements of liquid Fe–S alloys under high pressure (Huang et al., 2013; Morard et al., 2013) demonstrated that the outer core density profile is explained by Fe containing 10 wt.% S. The melting phase relations in the Fe–FeS system, in particular at the ICB pressure, are of great importance. In order for an Fe-rich phase to crystallize, the outer core liquid composition must be on the iron-rich side of the eutectic in the Fe–FeS binary system if sulfur is a predominant impurity element. They also constrain the partitioning of sulfur between the outer and inner core and the temperature at the ICB (see reviews by Li and Fei, 2007; Hirose et al., 2013). Alfè et al. (2002) predicted that the sulfur concentrations in coexisting liquid and solid Fe become almost identical at the ICB, but it has not been verified by experiments yet.

Fe and FeS exhibit a simple eutectic system at 1 bar, while intermediate compounds are formed at high pressures; Fe<sub>3</sub>S<sub>2</sub> above 14 GPa (Fei et al., 1997) and Fe<sub>2</sub>S and Fe<sub>3</sub>S above 21 GPa (Fei et al., 2000). The detailed binary phase diagram was examined to 40 GPa and above melting temperature by using a large-volume press (Stewart et al., 2007). Based on in-situ X-ray diffraction (XRD) measurements in a laser-heated DAC, the eutectic temperature and composition in the Fe–Fe<sub>3</sub>S system have been previously determined up to 123 GPa (Campbell et al., 2007; Chudinovskikh and Boehler, 2007; Morard et al., 2008, 2011; Kamada et al., 2010, 2012). Kamada and others obtained eutectic liquid compositions from ex-situ characterization of recovered DAC samples. These earlier studies have consistently reported that the sulfur concentration in the eutectic liquid reduces with increasing pressure (see Morard et al., 2014 for a review). The eutectic liquid compositions at the core pressure range have not been examined yet.

In this study, we extend melting experiments on the Fe–Fe<sub>3</sub>S system to 254 GPa using homogeneous starting materials. In order to determine the chemical compositions of coexisting liquid and solid, we focus on ex-situ textural and compositional characterizations of a sample recovered from a laser-heated DAC. Our results suggest that liquid Fe–S crystallizes the CsCl (B2)-type phase at 330 GPa when the liquid includes ≥6 wt.% S, lower than the

\* Corresponding author.

E-mail address: kei@elsi.jp (K. Hirose).

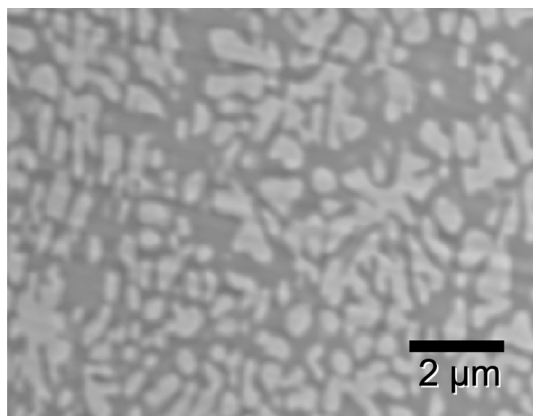


**Fig. 1.** Back scattered electron image of a starting material (Fe-14.5 wt.% S), a fine-grained mixture of Fe and FeS.

**Table 1**  
Compositions of starting materials.

	Fe (wt.%)	S (wt.%)	O (wt.%)
Fe-4.0 wt.% S	94.9(3)	4.0(3)	12(1)
Fe-5.9 wt.% S	94.6(9)	5.9(1)	0.7(0)
Fe-8.6 wt.% S	90.5(2)	8.6(1)	0.8(0)
Fe-10.3 wt.% S	88.9(5)	10.3(4)	0.7(0)
Fe-14.5 wt.% S	84.7(6)	14.5(6)	0.8(1)

Note: Numbers in parentheses represent one standard deviation.

10 wt.% S required to explain the core density deficit with sulfur as a single light alloying component. Moreover, the difference in sulfur concentration between coexisting liquid and solid Fe is too small to account for the density jump across the ICB.

## 2. Experimental methods

High pressure and temperature ( $P$ - $T$ ) conditions were generated in a laser-heated DAC using flat, single- and double-beveled diamond anvils with 40–300  $\mu\text{m}$  culets. Starting materials were the foils of Fe containing 4.0(3), 5.9(1), 8.6(1), 10.3(4), and 14.5(6) wt.% S (hereafter the number in parentheses indicates  $1\sigma$  uncertainty in the last digit), homogeneous mixtures of fine-grained Fe and FeS synthesized by an ultra-rapid quench method (Morard et al., 2011) (Fig. 1). Their chemical compositions and homogeneity were examined by a field-emission-type electron probe microanalyzer (FE-EPMA, JXA-8530F, JEOL) (Table 1). It was loaded into

a hole in a pre-indented rhenium gasket together with thermal insulation layers of  $\text{Al}_2\text{O}_3$ . As exceptions, in runs #11 and #12 performed above 254 GPa, we employed  $\text{SiO}_2$  glass for better thermal insulation and an MgO pressure marker placed between  $\text{SiO}_2$  and a diamond. After loading, a whole DAC was dried in a vacuum oven at 423 K, and subsequently the sample chamber was flushed with dry argon and squeezed in an argon atmosphere.

Pressure was determined at room temperature based on the Raman shift of diamond (anvil) (Akahama and Kawamura, 2004) except for runs #11 and #12 in which the equations of state of hexagonal close-packed (hcp) iron (Dewaele et al., 2006) and MgO (Tange et al., 2009) were used, respectively (Table 2). Note that since the atomic volume of sulfur is almost the same as that of iron above 180 GPa (Sata et al., 2010), substitution between sulfur and iron in the hcp phase does not alter cell parameters and thus calculated pressures (Sakai et al., 2012). The contribution of thermal pressure was then corrected. We added 5% per 1000 K to 200 GPa (Fiquet et al., 2010; Nomura et al., 2014). In run #12 of subsolidus experiment with in-situ XRD measurements, a pressure increase upon heating was found to be  $64 \pm 10\%$  of the isochoric thermal pressure (Andraut et al., 1998). We thus added 2.4% per 1000 K for runs #11–12. The overall pressure uncertainty may be  $\pm 10\%$  (except runs #11–12 with in-situ XRD data). The samples were heated at high pressures with a couple of 100 W single-mode Yb fiber lasers. Temperatures were measured by fitting thermal radiation spectrum to the Planck radiation function (Fig. 2). We have checked the spatial resolution using a 50  $\mu\text{m}$  diameter Re pinhole at the sample position. The derivative of the recorded edge showed that the full width at half maximum (FWHM) is 3 pixel (= 3  $\mu\text{m}$  on the sample) (Shen et al., 2001). Thus, the experimental temperature reported in this study is the average of temperatures in 3  $\mu\text{m}$  area at the solid/liquid boundary (Fig. 3a) (Ozawa et al., 2016; Hirose et al., 2017). The uncertainty in the present temperature determination may be  $\pm 5\%$ .

XRD data were collected for the sample in run #12 at BL10XU, SPring-8 using an X-ray beam with an energy of  $\sim 30$  keV. Angle-dispersive XRD spectra were collected on a flat panel detector (FPD) (Perkin Elmer) with typical exposure time of 1 s. A monochromatic incident X-ray beam was collimated to 2  $\mu\text{m}$  (FWHM). Visible fluorescence light induced by X-rays in a diamond was used to precisely align the laser-heated spot with an X-ray beam. Two-dimensional XRD images were integrated to produce a conventional one-dimensional diffraction profile using the IPAnalyzer software (Seto et al., 2010). Only in this run was the sample tem-

**Table 2**  
Experimental results.

Run #	Starting material	$P$ (GPa)	$T$ (K)	Duration (s)	Liquidus phase	Liquid			Solid Fe S (wt.%)
						S (wt.%)	C (wt.%)	O (wt.%)	
1	Fe-8.6 wt.% S	34(3)	1630(80)	30	Fe	12.5(12)			1.4(2)
2	Fe-8.6 wt.% S	45(5)	1740 <sup>b</sup>	60	subsolidus				
3 <sup>a</sup>	Fe-8.6 wt.% S	46(5)	1770(240) <sup>c</sup>	1	Fe	13.7(2)	0.3(12)	1.5(0)	1.4(2)
4 <sup>a</sup>	Fe-8.6 wt.% S	46(5)	1900(100)	120	Fe	14.1(3)	0.4(8)	1.9(3)	1.7(8)
5 <sup>a</sup>	Fe-14.5 wt.% S	47(5)	2030(100)	30	Fe <sub>3</sub> S	13.2(2)	−0.2(6)	1.5(0)	
6	Fe-8.6 wt.% S	60(6)	1910(100)	15	Fe <sub>3</sub> S + Fe	12.2(12)			
7	Fe-8.6 wt.% S	80(8)	2050(100)	15	Fe	11.3(11)			3.4(4)
8	Fe-8.6 wt.% S	130(13)	2910(150)	30	Fe <sub>3</sub> S	10.4(10)			
9 <sup>a</sup>	Fe-4.0 wt.% S	134(13)	2960(150)	3	Fe	9.1(1)	0.7(5)	1.8(1)	3.0(1)
10 <sup>a</sup>	Fe-10.3 wt.% S	200(20)	3320(170)	15	Fe <sub>3</sub> S	7.5(1)	0.6(5)	3.4(2)	
11	Fe-5.9 wt.% S	254(13)	3550(180)	20	Fe <sub>3</sub> S + Fe	5.7(3)			3.9(4)
12	Fe-5.9 wt.% S	278(14)	3570(180)	8	subsolidus				

Note: Numbers in parentheses indicate errors in the last digit.

<sup>a</sup> See Table A1 in Appendix for raw EPMA data. Sulfur and oxygen concentrations are obtained by subtracting C and  $\text{Al}_2\text{O}_3$  from the raw data.

<sup>b</sup> The highest temperature in the sample.

<sup>c</sup> Large uncertainty because of a larger temperature gradient.

Download English Version:

<https://daneshyari.com/en/article/5779918>

Download Persian Version:

<https://daneshyari.com/article/5779918>

[Daneshyari.com](https://daneshyari.com)